Selective oxidative degradation of azo dyes by hydrogen peroxide catalysed by manganese(II) ions

Jevan Bennett[a], Yusuf A. Miah[a], Dhimal S. Varsani[a], Enrico Salvadori[b]* and Tippu S. Sheriff[c]*

Manganese(II) ions catalyse the oxidative degradation of Calmagite (H_3CAL) dye in aqueous solution at 20±1°C in the pH range 7.5-9.0 using hydrogen peroxide (H_2O_2) as oxidant by a mechanism that involves strong complexation to the MnII centre. It is proposed that [MnIII(CAL)(O2H)]– i.e. a dye coordinated hydroperoxyl (O_2H^-) MnIII complex is formed and bleaching of the dye is initiated by an electron-transfer to MnIII, with the binding of H_2O_2 being the rate determining step. At pH 9.0 in (bi)carbonate, HCO_3^-, H_3CAL is rapidly bleached via the in situ formation of coordinated peroxycarbonate (HCO_4^-); a TOF (TOF = moles of dye bleached per mole of manganese per hour) of ~5000 hr–1 can be achieved. The bleaching of the related azo dyes Orange II and Orange G is different because, unlike Calmagite, they lack an o,o-dihydroxy motif so are unable to complex strongly to MnII and no oxidation to MnIII occurs. At pH 8.0 (phosphate buffer) Orange II and Orange G are not bleached but bleaching can be achieved at pH 9.0 (HCO_3^- buffer); the rate determining step is dye coordination and it is proposed bleaching is achieved via an outer-sphere oxygen atom transfer. Mechanisms for dye bleaching at pH 8.0 and pH 9.0 are proposed using data from EPR, UV/VIS and ESI-MS. MnII/ H_2O_2/ HCO_3^- form a potent oxidising mixture that is capable of removing stubborn stains such as curcumin.

Introduction

Higher valent manganese complexes have been implicated in a wide variety of natural, biomimetic and synthetic processes involving both substrate oxidation and reduction including photosynthetic water oxidation, dioxygen activation and reduction to hydrogen peroxide (H_2O_2), epoxidation and bleaching. The use of H_2O_2 as the terminal oxidant in oxidation processes in favoured due to its environmentally benign nature, the byproduct in its use being water.[1] From a green chemistry viewpoint it is the ideal oxidant with an atom efficiency (47%), bettered only by dioxygen (O_2, 50%), but exhibiting better reaction kinetics. Large scale uses of H_2O_2 include the bleaching of paper in the wood pulp industry, as a detergent in the form of perborates and percarbonates in washing powders, and in the chemical treatment of water systems.[2]

The treatment of wastewaters from dye manufacturers and the textile processing industries is a challenge[3] with azo dyes which contain the –N=N– moiety being particularly problematic as they account for 70% of textile dyestuffs and are also chemically stable.[4] It has been estimated that 128 tonnes of dye materials are released daily into the environment and by the nature of their use they are designed to be resistant to environmental degradation.[4, 5] Thus they are non-biodegradable under aerobic conditions and under anaerobic conditions produce hazardous intermediates.[6] The oxidative degradation of Orange II (sodium 4-[(2-hydroxy-1-naphthyl)azo]benzene sulfonate, Scheme 1), a model azo dye substrate, has been described by van Eldik and co-workers using H_2O_2 with either MnII salts[7] or MnII(bipy)2 complexes[8] in carbonate (HCO_3^-) buffer in the pH range 8 – 10, and MnII salts using commercial peracetic acid[9] at pH 9.5.
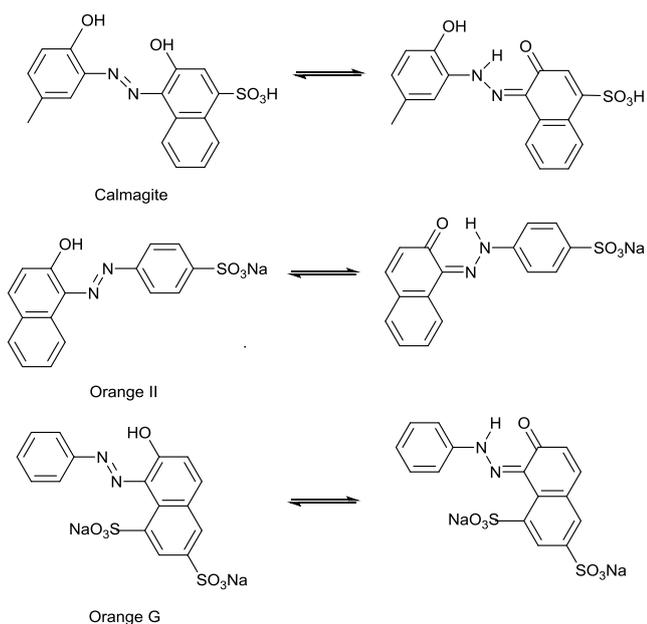
Scheme 1 Azo-hydrazone tautomerism of Calmagite, Orange II and Orange G in aqueous solution.

In the use of MnII salts, van Eldik found that only the HCO3– buffer system was able to oxidatively degrade Orange II and he proposed a mechanism involving peroxycarbonate (HCO4–) that is formed when H2O2 reacts with HCO3– (Scheme 2).
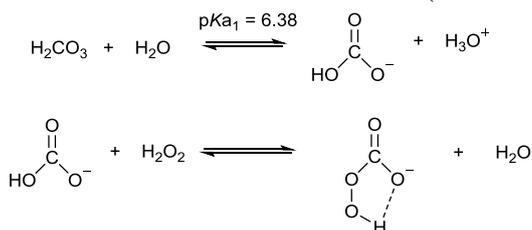
Scheme 2: Mechanism for the formation of peroxycarbonate from carbonate and hydrogen peroxide.

HCO4– ions are reported to be several orders of magnitude more reactive than H2O2 towards nucleophilic substrates[10] because carbonate (CO32–) is a better leaving group than hydroxide (OH–)[11]. In the presence of MnII, HCO4– is complexed to produce a MnII-□2-peroxycarbonate complex which van Eldik proposes then breaks down to MnIV=O that is the active catalyst in the oxidatative degradation of Orange II through the transfer of an oxygen atom. Van Eldik suggests this transfer is assisted by the weak binding of Orange II to MnII and that this complexation stabilises the MnII-□2-peroxycarbonate pre-catalyst (Scheme 3).

Scheme 3 Proposed mechanism for the oxidative degradation of O II via the in situ formation of MnIV=O species.
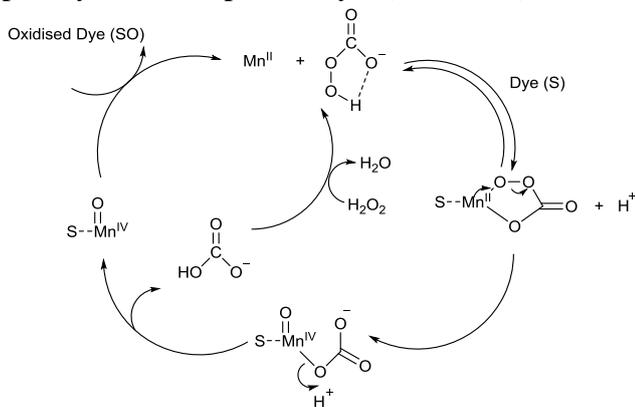
We have previously described the complete degradation of Calmagite (3-hydroxy-4-(2-hydroxy-5-methylphenylazo)naphth-alene-1-sulfonic acid) under ambient conditions using in situ generated H2O2 catalysed by MnII ions at pH 8.0 in N-2-hydroxyethylpiperazine-N'-3-propanesulfonic acid, EPPS, buffer.12 Under these conditions Orange II and Orange G (3-hydroxy-4-(phenylazo)naphthalene-1,5-disulfonate, disodium salt) were not bleached and it was suggested that this was because these substrates lacked an additional hydroxyl group ortho to the azo group (Scheme 1) thus resulting in weaker binding to MnII. The presence of Tiron (1,2-dihydroxybenene-3,5-disulfonate disodium salt, monohydrate, Na2TH2·H2O), with [Tiron]/[dye] ~15 was required for efficient in situ generation of H2O2. The mechanism for oxidative degradation of Calmagite was proposed to involve a MnIII-OOH species within a highly oxidizing MnIII Tiron-quinone complex, with no evidence of MnIV=O species by EPR. While the in situ generation of H2O2 from O2 for dye bleaching is highly attractive, the presence of hydroxylamine (NH2OH) in stoichiometric amounts as the reducing substrate and Tiron as an essential co-ligand makes the application of this system unsuitable for wastewater treatment. We were therefore interested to use simple MnII salts in the presence of added H2O2 to investigate the oxidative degradation of Calmagite, Orange II and Orange G as model substrates in the pH range 7.5-9.0 using both phosphate and carbonate buffer systems. These substrates were chosen because they represent a range of MnII binding abilities viz. Calmagite >> Orange II ~ Orange G. In this study we wish to detect the differences in the mechanisms of dye bleaching at pH 8.0 (phosphate) and pH 9.0 (carbonate) and to determine if we could detect MnIV=O species in the latter system by EPR, as previously reported by van Eldik.7 The use of H2O2 provides a cheap and more atom economic oxidant compared to peracetic acid (and other peracids) and hypochlorite (which also releases chlorine into the environment). There are a wide range of metal systems known to catalyse the degradation of azo dyes but these are associated with elaborate ligand systems which add expense and chemical demands in the treatment of wastewater. The use of simple MnII salts in these systems is viewed as benefical in terms of economics and atom efficiency, thus realising the goals of green chemistry.

Results and Discussion

Calmagite

Fig. 1 is a visible spectrum scan (400-700 nm) showing the change in absorbance of an aqueous solution of Calmagite (H3CAL henceforth referred to as 'CAL', 0.100 mM, ⬜max ~540 nm) at pH 8.0±0.1 (phosphate buffer) and 20±1°C in the presence of added H2O2 (50.0 mM) and aqueous Mn2+ (5.00 ⬜M) as catalyst (initial molar ratio Mn: CAL: H2O2 = 1: 20: 10,000).
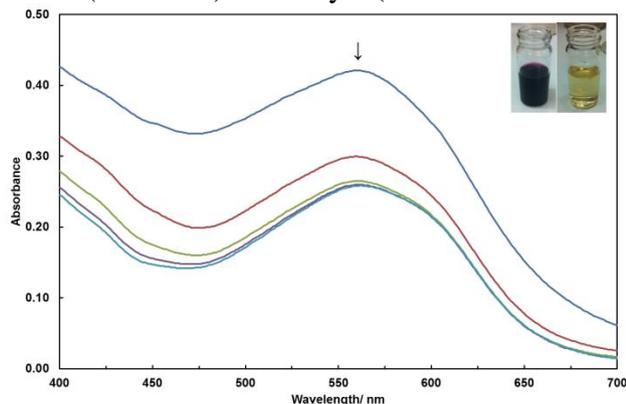
Fig. 1 The change in absorbance spectrum of CAL at 5 min intervals from t = 0 to t = 20 min at 20±1°C with [MnCl2·4H2O] at 5.00 □M. Initial [CAL] and [H2O2] were 0.100 mM and 50.0 mM respectively. The pH was 8.0±0.1 (50 mM, phosphate buffer). Insert: The colour of CAL before (left) and after (right) the reaction.

There is an initial rapid decrease in [CAL] (t = 0-5 min) followed by smaller decreases [CAL] with time. At the end of the 20 min period there is no trace of the purple colour in the reaction solution (Fig. 1 (insert)). Previous studies on the in situ generation of H2O2 and CAL dye bleaching were carried out at pH 8.0 using the non-coordinating, biological, EPPS buffer; the use of phosphate buffer here seems not to have any detrimental affect on the ability of the MnII to catalyse this reaction suggesting that phosphate can easily be displaced by CAL in coordination sites around MnII. In this coordinated state it would be expected that the azo form of CAL would dominate over the hydrazine tautomer (Scheme 1) with electron density concentrated on the oxygen atom.12 The effect of the variation of [MnII] between 0 and 100 □M on the oxidative degradation of CAL is shown in Fig. 2 and ESI1†.
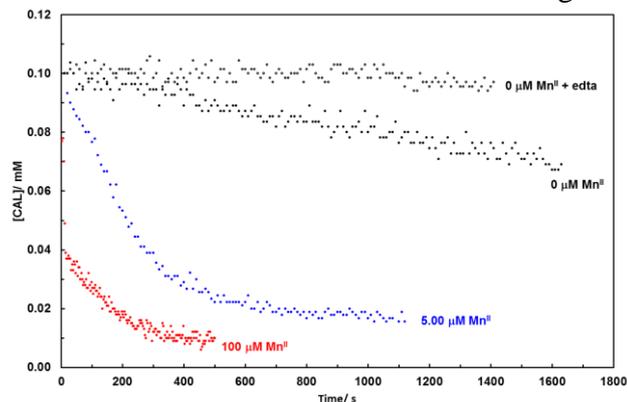
Fig. 2 The change in [CAL] with time monitored at 540 nm and at 20±1°C with [MnCl2·4H2O] varied from 0, and with added ethylenediaminetetraacetic acid (EDTA, 1.00 mM), to 100 □M. Initial [CAL] and [H2O2] were 0.100 mM and 50.0 mM respectively. The pH was 8.0±0.1 (50 mM, phosphate buffer).

In the absence of added MnII there is only slow bleaching of CAL and this is stopped almost completely in the presence of ethylene diamine tetra-acetate (EDTA4–, 1.00 mM), and is presumably due to the presence of adventitious MnII. [MnII] as low as 0.500 □M catalyses the bleaching of CAL. At 5.00 □M and lower concentrations of MnII, the rate of bleaching is independent of the [CAL] ([CAL]/[MnII] > 20 initially) suggesting that coordination of CAL to MnII is fast. With an excess of H2O2, there is a first order dependency on [MnII] (ESI1†) with the pseudo first order rate constant calculated to be 3.9×10^{-2} s^{-1} with a TOF of ~140 hr^{-1}. There are small increases in the rate of CAL bleaching when the pH is raised from 7.5 to 8.0 and then 8.5. This is consistent with an increase in the [HO2–] (pKa H2O2 = 11.6714) with relative [HO2–] at pH 7.5, 8.0 and 8.5 of 1: 3.3: 10 respectively and this suggests that the coordination of H2O2 may be the rate determining step. Unsurprisingly, the rates of reaction and TOF observed here are much faster than that observed previously using in situ generated H2O2 (from O2) where the equilibrium concentration of oxidant is lower and competition for binding sites around the manganese greater due to the presence of reducing substrate hydroxylamine (NH2OH, 100 mM) and ligand Tiron (1.50 mM).13 A first order dependency of CAL bleaching on [H2O2] (ESI2†) and [CAL] (ESI3†) was observed but the rate of bleaching was found to be independent of the [phosphate]. To gain insight into the chemical species formed during the reaction cycle, we employed electron paramagnetic resonance (EPR) spectroscopy. For semi-integer spin systems, e.g. MnII S = 5/2, the highest EPR sensitivity (i.e. higher transition probability) is achieved with the external field and the microwave field perpendicular to each other. For integer spin systems, e.g. MnIII S = 2, the transition probability drops to zero when the external field and the applied magnetic field are perpendicular, but is largest when they are parallel. The EPR spectrum (X-

band, perpendicular mode) of a solution of MnII (100 ☐M) at pH 8.0 (phosphate buffer) containing H2O2 (50.0 mM) revealed the characteristic six-line spectrum (ESI4†) of the high-spin ion (S = 5/2) coupled to the manganese nucleus (55Mn, I = 5/2). When the EPR experiment was repeated in both perpendicular and parallel modes after the addition CAL (0.100 mM), the six line spectrum (perpendular mode) was still present (Fig. 3) but there was no evidence for the presence of MnIII species (parallel mode) nor was there any signal at ~150 mT (g ~ 4.5) in perpendicular mode indicative of MnIV=O (S = 3/2).
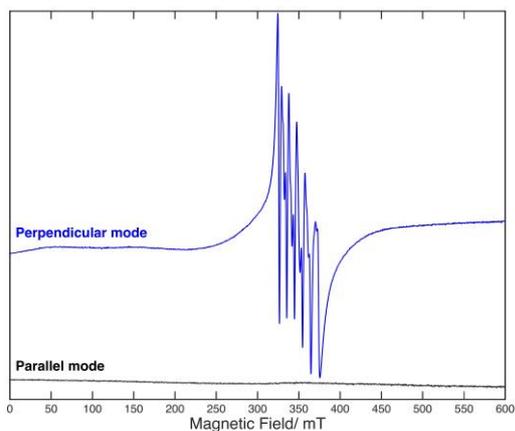
Fig. 3 X-band EPR spectra of MnCl2·4H2O (100 ☐M), H2O2 (50.0 mM) and CAL (0.100 mM) at pH 8.0 (50 mM, phosphate buffer) in both perpendicular (9.65 GHz) and parallel (9.41 GHz) modes. EPR conditions: 10 K, 2 mW microwave power, modulation amplitude 0.5 mT.

On the other hand, MnIII was observed in the EPR (parallel mode) when an aqueous solution of MnCl2·4H2O (0.10 mM) was added to aqueous Tiron (~0.30 mM) at pH 8.0 (50 mM EPPS) to form [MnIII(T)2]5− in situ by aerial oxidation15 (Fig. 4). The measured signal is faint and does not display any resolved hyperfine structure, nonetheless its resonance position (g ~ 8.1) is consistent with previously reported MnIII signals.16
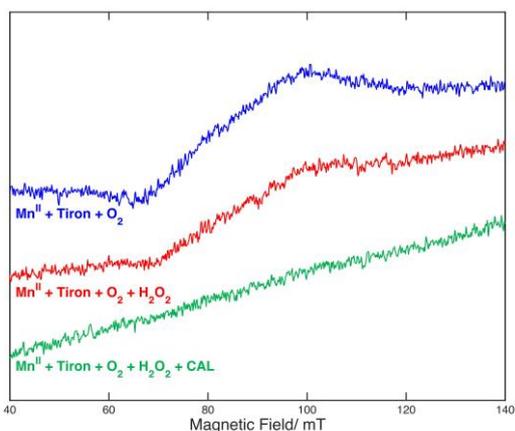
Fig. 4 X-band EPR spectra of MnCl2·4H2O (100 ☐M) and Tiron (~0.30 mM) at pH 8.0 (50 mM, phosphate buffer) followed by the addition of H2O2 (50.0 mM) and then CAL (0.100 mM). EPR conditions: Parallel mode, 9.41 GHz, 10 K, 2 mW microwave power, modulation amplitude 0.5 mT.

When H2O2 (50 mM) was added the MnIII signal was still observable, whereas when CAL (0.100 mM) was introduced the signal disappeared. This suggests that in the presence of excess CAL (and H2O2) the equilibrium [MnIII] is low as it is reduced to MnII due to a one-electron transfer from bound CAL, which in turn initiates the oxidative degradation of the dye. Returning to the added H2O2

system (without Tiron), Fig. 5 shows the results of a semi-quantitative EPR study at pH 8.0 (phosphate buffer) in which the height of the peak at lowest magnetic field (~315 mT) was used as a proxy for [MnII] present.

When only H2O2 was added there was no observable change in [MnII], indicating that this state is
10 quite stable despite the presence of an excess of a strong oxidant. When the experiment was repeated with CAL but no H2O2, there was a large decrease in MnII signal, possibly due to the formation of the MnIII-CAL complex. Similar to Mn/Tiron system, this d4 state is presumably stabilised by the CFSE now gained by the coordination of a relatively strong-field ligand. With both CAL and H2O2 present, there is a ~50% reduction in MnII signal, and the assumed ~50% MnII/MnIII present is due to the
15 presence of both reduced and oxidised Mn species as coordinated CAL is 1-e– oxidised. None of the EPR data shows any evidence of radical species and when CAL bleaching was repeated in the presence of an excess of the radical scavenger 2,4,6-tri-tert-butylphenol there was no reduction in the rate of oxidative degradation suggesting that the mechanism does not involve radical species e.g. ●OH and ●O2H. Fig. 6 shows an UV/VIS spectrum of a mixture of MnII with H2O2 (pH 8.0, phosphate
20 buffer) exhibiting an absorption peak at ~240 nm due to the formation of a MnII-hydroperoxo complexref; this peak is substantially broadened and red shifted on the addition of CAL and the peak decreases only slowly over a period of 30 min. The change in the UV part of the spectrum on addition of CAL is presumably due to the binding of CAL to the metal centre and subsequent oxidation of MnII to MnIII and the very small changes in the UV region thereafter suggests that as CAL is oxidatively
25 decomposed there is fast coordination of remaining CAL to the metal centre, with rapid mineralisation of the initial oxidation products of the dye.
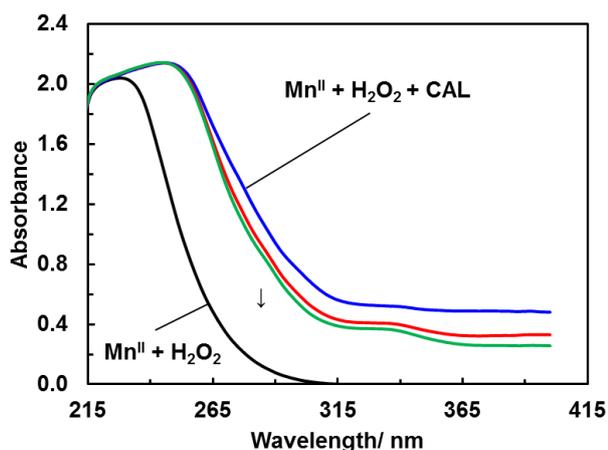
Fig. 6 UV/VIS spectrum of a CAL bleaching solution at 20±1°C before and after the addition of CALwith then repeat scans until t = 30 min. [MnCl2·4H2O] was 5.00 □M and the initial [CAL] and [H2O2] were 0.100 mM and 50.0 mM respectively. The pH was 8.0±0.1 (50 mM, phosphate buffer).

An ESI-MS chromatogram (ESI5†) of a CAL bleaching solution shows high intensity peaks at m/z 450.3 and m/z 484.8 that correspond to [MnIII(NaCAL)(H2O)]+ and [MnIII(NaHCAL)(O2H)(H2O)]+ species respectively; these peaks were absent when MnII was not added. Taken together, the kinetic, UV/VIS, EPR and MS data are consistent with a mechanism for CAL bleaching that involves the oxidative degradation of coordinated CAL in the presence of coordinated HO2– at a MnIII centre (eqn (1)-(4)).

MnII + H3CAL ⇌ [MnII(CAL)]– + 3H+   (1)
2[MnII(CAL)]– + ½O2 + 2H+ ⇌ 2[MnIII(CAL)] + H2O   (2)
[MnIII(CAL)] + H2O2 ⇌ [MnIII(CAL)(O2H)– + H+   (3)
[MnIII(CAL)(O2H)– → MnII + CAL oxid. products   (4)
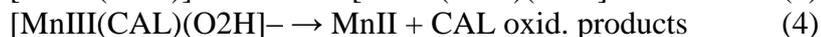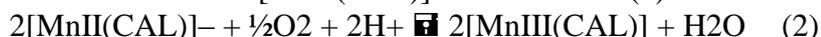
Step (4) can be considered to be fast given the lack of observable MnIII in the EPR parallel mode. The role of H2O2 as the terminal oxidant in this system is interesting in that it could be used simply to reduce MnIII back to MnII in a catalase-like process, but the system is probably more complicated with coordinated peroxide taking an active role in the initiation of CAL breakdown. The presence of excess H2O2 in solution is probably responsible for   further oxidation of the initial oxidation product resulting in complete the mineralisation of the dye.13 Oakes et al have also proposed that specific complexation of CAL is a requirement for its oxidative degradation when using peroxosulfate as terminal oxidant and suggested that this may occur via a one-electron transfer from MnIII involving an inner-sphere mechanism.17 The rate of loss of CAL is given by eqn. (5).

–d[CAL]/dt = k1[Mn(CAL)(O2H)]   (5)

When there is an excess of H2O2 in solution and the [CAL] is large, the rate of CAL bleaching can be expressed as eqn. (6).

–d[CAL]/dt = kobs[MnII]   (6)

We were interested to investigate the effect of Tiron on CAL dye bleaching at pH 8.0 (50 mM EPPS) as this ligand was previously found to be essential not only for the in situ generation of H2O2 but also for CAL bleaching.9 In the absence of added Na2CO3 with [Tiron4–] at 1.50 mM (Mn: Tiron4–: CAL: H2O2 = 1: 30: 2: 500), there is a clear lag period during which time CAL bleaching is inhibited. However, this lag period is reduced when sodium carbonate was added and there were step-wise reductions as the [Na2CO3] is increased to 50.0 mM (Fig. 7).
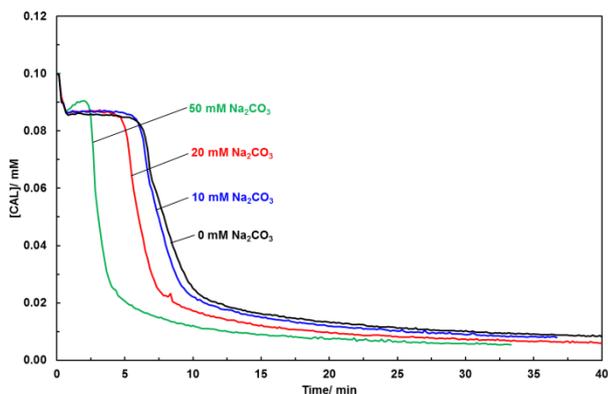
Fig. 7 The change in [CAL] with time monitored at 535 nm and at 20±1°C in the presence of Tiron with [Na2CO3] varied from 0 to 50 mM and with [MnCl2·4H2O] at 50.0 ☐M. Initial [CAL], [H2O2] and [Tiron] were 0.100 mM, 50.0 mM and 1.50 mM respectively.The pH was 8.0±0.1 (50 mM, N-2-hydroxyethylpiperazine-N'-3-propanesulfonic acid, EPPS, buffer).

In the absence of added Na2CO3 these results are consistent with the need for CAL to be bound to MnII for bleaching to occur and that Tiron4– can initially compete effectively for binding sites around the metal. When Na2CO3 was added the in situ formation of peroxycarbonate (HCO4–) is itself able to compete with Tiron for binding sites around MnII ([HCO4–]/[Tiron]~6.7-33) and this leads to a progressive reduction in the lag period as the [HCO4–] is increased.

Fig. 8 shows a comparison of the rates of CAL bleaching at pH 8.0±0.1 (50 mM phosphate) and at pH 9.0±0.1 (50 mM carbonate, ☐max ~608 nm) with [MnII] at 0.500 ☐M.
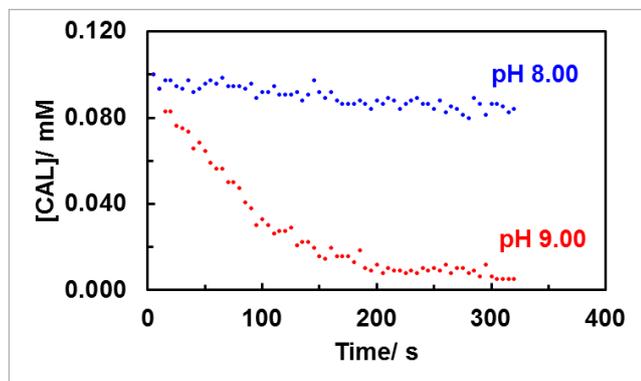
Fig. 8 The change in [CAL] with time monitored at 535 nm at pH 8.0±0.1 (50 mM, phosphate buffer) and 608 nm (50 mM, carbonate buffer) at 20±1°C with [MnCl2·4H2O] at 0.500 ☐M. Initial [CAL] and [H2O2] were 0.100 mM and 50.0 mM respectively.

The TOF at pH 9.0 is calculated to be ~5000 hr–1 which is ~35 times larger than at pH 8.0. These higher bleaching rates cannot be solely accounted for by the higher [HO2–] at this pH (~10 times higher than at pH 8.0) and it would appear that the binding of HO2– at pH 9.0 is much faster than the binding of H2O2 in phosphate buffer at pH 8.0 and this leads to the faster formation of [MnIII(CAL)(O2H]– and can account for the faster bleaching rate under these conditions (Scheme 4).
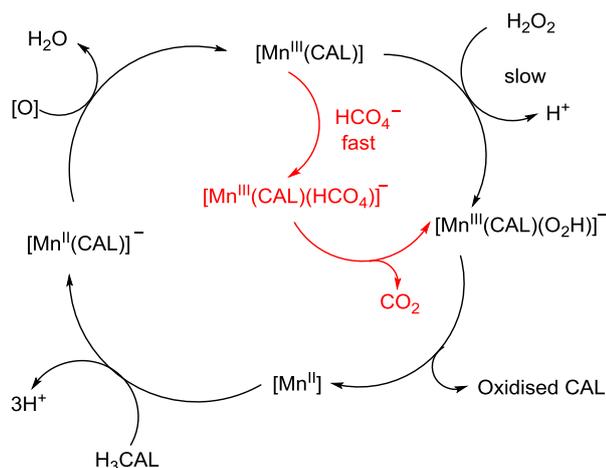
Scheme 4 Proposed mechanism for the oxidative degradation of CAL at pH 8.0 (phosphate, black) and pH 9.0 (carbonate, red).

The reaction at pH 9.0 was much more sensitive to adventitious MnII with slow bleaching in the absence of added MnII; this activity was again effectively reduced to zero in the presence of EDTA4– (1.00 mM). Thus while carbonate/peroxide mixtures resulting in the in situ formation of HCO4– may be viewed as strongly oxidising, accelerated rates under ambient conditions may only be observed in the presence of metal ions.

The addition of Tiron to CAL bleaching at pH 9.0 (EPPS buffer) with varying [Na2CO3] is shown in Fig. 9.
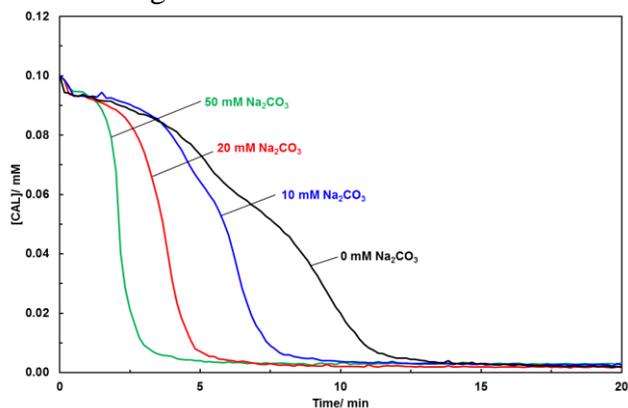
Fig. 9 The change in [CAL] with time monitored at 608 nm and at 20±1°C in the presence of Tiron with [Na2CO3] varied from 0 to 50 mM and with [MnCl2·4H2O] at 50.0 ☐M. Initial [CAL], [H2O2] and [Tiron] were 0.100 mM, 50.0 mM and 1.50 mM respectively. The pH was 9.0±0.1 (50 mM, N-2-hydroxyethylpiperazine-N'-3-propanesulfonic acid, EPPS, buffer).

In general the lag periods were found to be smaller than at pH 8.0 and the rates of dye bleaching faster with saturation at ~50 mM Na2CO3 consistent with the maximum stoichiometric amount of HCO4– that can be formed in solution at pH 9.0 (Scheme 2).

Orange II and Orange G

Fig. 10 and Fig. 11 show repeat UV/VIS scans (300-700 nm) of aqueous solutions of Orange II (O II, 0.100 mM, ☐max ~484 nm) and Orange G (O G, 0.100 mM, ☐max 486 nm) respectively at pH 9.0±0.1 (carbonate buffer) and at 20±1°C in the presence of added H2O2 (50.0 mM) and aqueous Mn2+ (5.00 ☐M) as catalyst.
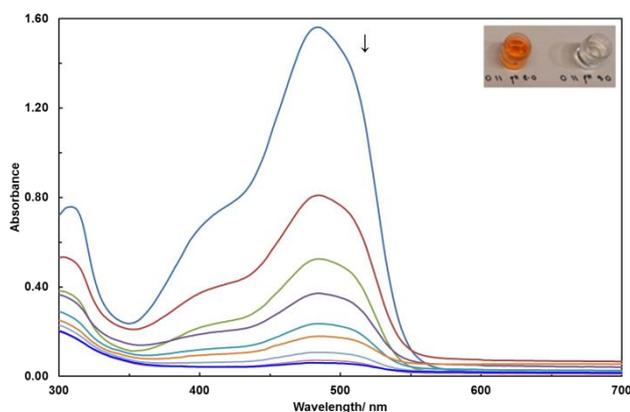
Fig. 10 The change in [O II] from t = 0 to t = 10 min and then at 5 min intervals to 45 min monitored at 484 nm and at 20±1°C with [MnCl2·4H2O] at 5.00 □M. Initial [O II] and [H2O2] were 0.100 mM and 50.0 mM respectively. The pH was 9.0±0.1 (50 mM, carbonate buffer). Insert: The colour of O II after attempted oxidative degradation at pH 8.0 (left, no change) and at pH 9.0 (right, completely bleached).
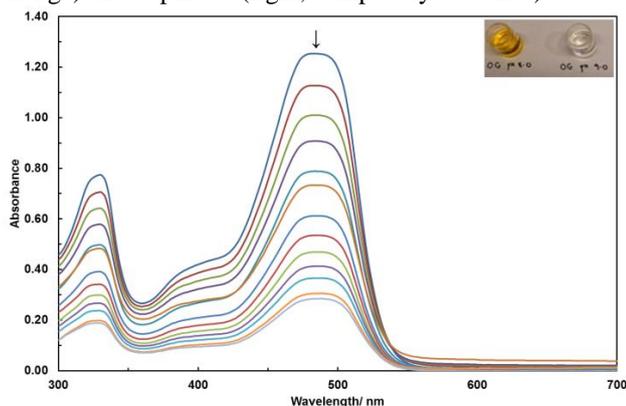
Fig. 11 The change in [O G] from t = 0 to t = 60 min at 5 min intervals to 45 min monitored at 486 nm and at 20±1°C with [MnCl2·4H2O] at   5.00 □M. Initial [O G] and [H2O2] were 0.100 mM and 50.0 mM respectively. The pH was 9.0±0.1 (50 mM, carbonate buffer). Insert: The colour of O G after attempted oxidative degradation at pH 8.0 (left, no change) and at pH 9.0 (right, completely bleached).

For these dyes not only is there a decrease in the absorbance of the broad colour chromophore centered at ~484 nm (and shoulder at ~500 nm in the case of O II) but also a decrease in the absorbance of the naphthalene ring absorbance at ~320 nm, suggesting complete mineralisation of the dyes. These results are different to that obtained by Nunes et al using manganese(II) hydroxybenzyl-pyridyl-diamine complexes in the oxidative degradation of methyl orange where there was an increase in the absorbance at ~330 nm attributed to the formation of the amine oxide.[18] When the bleaching of O II and O G was attempted at pH 8.0 (phosphate or EPPS, Fig. 10 and Fig. 11, inserts), there was no change in the colour of the dyes over a period of ~30 min. Van Eldik also reported that O II was not bleached in any other of a range of buffer systems (including phosphate) in the pH range 8-9.7 Fig. 12 and Fig. 13 show the effect of the variation of [MnII] between 0 and 100 □M on the bleaching of O II and O G respectively.
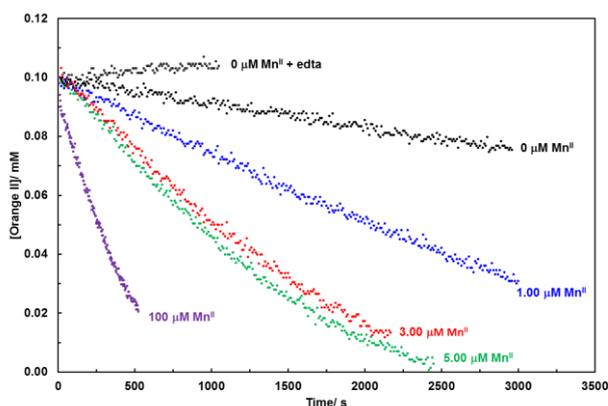
Fig. 12 The change in [O II] with time monitored at 484 nm and at 20±1°C with [MnCl2.4H2O varied from 0 to 100 □M. Initial [O II] and [H2O2] were 0.100 mM and 50.0 mM respectively. The pH was 9.0±0.1 (50 mM, carbonate buffer).
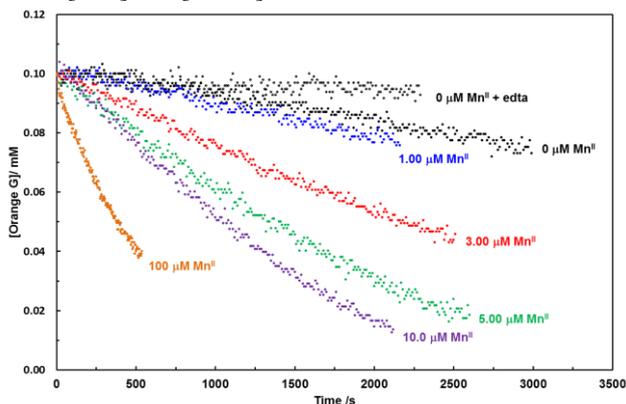
Fig. 13 The change in [O G] with time monitored at 486 nm and at 20±1°C with [MnCl2.4H2O varied from 0 to 100 □M. Initial [O II] and [H2O2] were 0.100 mM and 50.0 mM respectively. The pH was 9.0±0.1 (50 mM, carbonate buffer).

In the absence of added MnII there is slow adventitious MnII bleaching of the dyes and this is virtually stopped in the presence of EDTA4– (1.00 mM). [MnII] as low as 1.00 □M catalyses the bleaching of the dyes and there is an unexpected ~1/2 order dependency on [MnII] (ESI6†) for both dyes with pseudo first order rate constants for O II and O G calculated to be 1.4×10^{-2} s^{-1} and 6.2×10^{-3} s^{-1} respectively giving TOFs of ~50 hr^{-1} and ~20 hr^{-1} respectively. These TOFs is ~100 times lower than that for CAL bleaching at pH 9.0 using carbonate buffer and this reflects the lower binding constants of O II and O G to MnII compared to CAL. Again, rather unexpectedly there are similar fractional order dependencies on [H2O2] (ESI7†) and HCO3– (ESI8†) of ~1/2 and ~3/4 for both dyes. These fractional order dependencies suggest that the catalytic system is complicated and merit further investigation. A UV/VIS spectrum of solution an O G bleaching solution is shown in Fig. 14. Before the addition of O G there is a peak centered at ~245 nm presumably due to the MnII-□2-peroxycarbonate complex. This peak is broadened and red shifted on the addition of O G and there is then a decrease in the absorption of this peak over a period of 60 min. At the end of 60 min (when all the O G would be exhausted), the UV/VIS spectrum is almost identical to the spectrum containing MnII and H2O2 only indicating that the change in spectrum is reversible and is due to the weak binding of O G to the metal centre. A very similar spectrum was obtained with O II. These changes are presumably due to the formation and subsequent decomposition of a manganese-peroxycarbonate species.
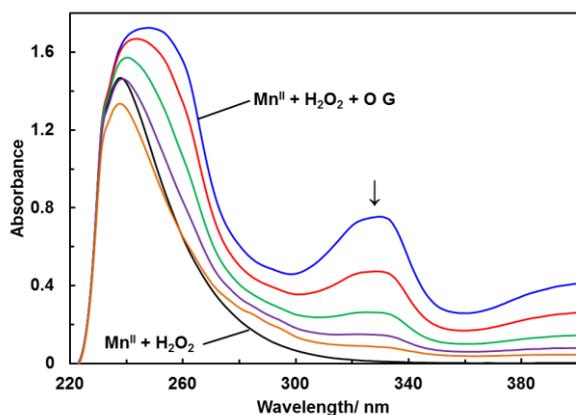
Fig. 14 UV/VIS spectrum of a O G bleaching solution at 20±1°C before and after the addition of O G with then repeat scans until t = 60 min. [MnCl2·4H2O] was 5.00 □M and the initial [O G] and [H2O2] were 0.100 mM and 50.0 mM respectively. The pH was 9.0±0.1 (50 mM, carbonate buffer).

The EPR spectrum of a solution of MnII (100 □M) at pH 9.0 (HCO3– buffer) exhibits the usual six-line pattern, which appears to be broadened and exhibit distinctive anisotropy as compared to its counterpart in phosphate buffer, presumably because of the coordination of the HCO3– anion (ESI4†). On addition of H2O2   (50.0 mM) the six-lines pattern sharpens up but reduces, however there is no evidence for a signal at g ~ 4.5 (~150 mT) characteristic of MnIV=O. This six line spectrum is again prominent on the addition O II (0.100 mM), yet there is no evidence for the formation of MnIV=O species at 150 mT (g ~ 4.5) in perpendicular mode nor MnIII in parallel mode at 100 mT (ESI9†), nor any decrease in the [MnII] in a bleaching solution containing O II, as judged from the height of the peak at lowest magnetic field at ~315 mT (ESI10†). These results are at odds with the mechanism proposed by van Eldik who implicated MnIV=O species for O II bleaching in carbonate buffer at pH 8.5.7 However, van Eldik did not carry out any EPR studies in his work and so the involvement of MnIV=O in these systems is somewhat speculative. A similar set of EPR spectra were obtained when O II was replaced by O G. This work suggests that MnIV=O is either not formed or is a very transient species in this system. When O II and O G bleaching were repeated in the presence of an excess of 2,4,6-tri-tert-butylphenol there was no reduction in the rate of dye bleaching. This implies that the mechanism does not involve radical species. The rate determining step in the oxidative degradation of O II and O G is the coordination of the dye substrate to MnII. Analogous to Scheme 4 for CAL in the presence of carbonate, a mechanism can be proposed for the bleaching of O II and OG that in the last step involves an oxygen atom transfer to dye substrate (S) from coordinated HO2– (Scheme 5).
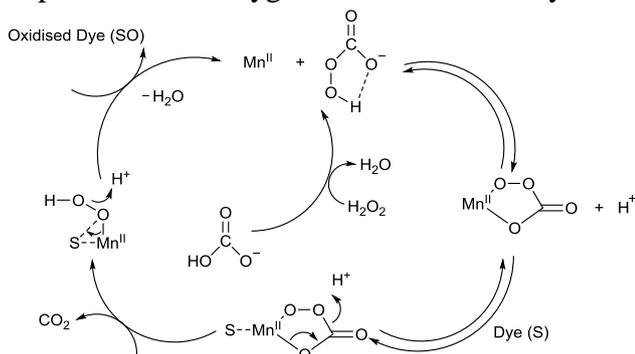
Scheme 5 Proposed mechanism for the oxidative degradation of O II and O G via the in situ formation of MnII–O–O–H species.

The final step in the oxidation of dye substrate is similar to the mechanism proposed by van Eldik but in this outer coordination sphere process there is no requirement for the formation of MnIV=O species.

The fractional order dependencies on MnII, H2O2 and HCO3– may be explained by the complex series of equilibria in the formation of HCO4– and its consumption in the release of CO2 and in the formation of MnII-OOH. This mechanism does require a change in oxidation state of MnII and fits the EPR data obtained. Manganese is effectively acting as a binding centre enabling transfer of an oxygen atom from bound oxidising agent to bound dye substrate. The differences in the rate of dye bleaching and TOF values between CAL, O II and   O G at pH 9.0 (carbonate buffer) may be explained by the differences in their complexation to the manganese centre in the stabilisation of the in situ formed dye-manganese-peroxybarbonate species. The better a dye is able to bind to MnII and stabilise this species (with oxidation to MnIII with CAL) the greater the rate of oxidative degradation (Table 1).

Table 1 Summary of the rate constants (k) and turnover frequencies (TOF) at 20±1°C for the manganese(II) catalysed oxidative degradation of dyes using hydrogen peroxide. In all cases the initial [Dye] was   0.100 mM, [buffer] was 50 mM, [H2O2] was 50.0 mM and [MnCl2·4H2O] was 5.00 ☐M.

Fig.	Dye	pH/ buffer	k/ s^{-1} (TOF/ hr^{-1})[1]
1/ESI1	Calmagite	8.0/ phosphate	3.9×10^{-2} (140)
8	Calmagite	9.0/ carbonate	1.4×10^{0} (5000)
12/ESI6	Orange II	9.0/ carbonate	1.4×10^{-2} (50)
13/ESI6	Orange G	9.0/ carbonate	6.2×10^{-3} (20)

[1]TOF = turnover frequency = moles of dye oxidised per mole of MnCl2·4H2O per hour.

We have determined the stability constants for the complexation of MnII with O II and O G based on the reduction in the wavelength maxima for 5.00×10^{-5} M concentrations of the dyes on the addition of $1.00 - 6.00 \times 10^{-5}$ M concentrations of MnCl2·4H2O (ESI11†). The log stability constants for O II and O G were calculated to be identical at 4.31 which is very close to a previously reported value 4.57 for O II. The log stability constant for the coordination of MnII to CAL has a value of 11.519. Therefore the binding constant of CAL for MnII is ~107 greater than that for O II and O G and this can account for its ability to be rapidly bleached by an inner-sphere electron transfer from MnIII. With O II and O G their weak binding ability to MnII means that MnIII is most likely not formed they cannot be bleached at pH 8.0 (phosphate buffer); at pH 9.0 (carbonate buffer) oxidative degradation occurs through a more difficult outer-sphere oxygen atom transfer. The lower bleaching rates observed with O G compared to O II could be due to the presence of two sulfonate groups in its structure that reduce is binding ability still further by reducing the electron density at the phenolic oxygen anion and possibly the lone pairs of electrons on the two nitrogen atoms.

Conclusions
This study has shown that a simple MnII salt is able to efficiently activate H2O2 and H2O2/HCO3– mixtures to oxidatively degrade model dyes under ambient conditions. Dyes which strongly complex with the metal e.g. CAL may be degraded by a one-electron oxidation reactions at both pH 8.0 (phosphate) and pH 9.0 (carbonate). O II and O G are not bleached at pH 8.0 (phosphate) but can be degraded at pH 9.0 (carbonate) through the in situ formation of [S---MnII(OOCO2)] and oxidation occurs through an oxygen atom to the dye substrate from   [S---MnII(OOH)]. The differences in the rates of bleaching between CAL (pH 8.0, phosphate) and O II (and O G, pH 9.0 carbonate) can be compared (ESI12†) through successive additions of fresh portions of CAL and O II

to the reaction solutions which also show only small reductions in the rates of dye bleaching at each step, suggesting that the integrity of the catalyst is preserved during these repeated cycles. Work in these laboratories has shown that even difficult to remove stains such curcumin (curry stain) may be degraded using H_2O_2/HCO_3^- mixtures at pH 9.0 which provide a potent oxiding medium in the presence of added Mn^{II}. The tailoring of dye bleaching to the nature of the oxidising reagent has important implications in laundry formulations in the need to remove stain molecules while not bleaching fabric dyes. One application of these findings is the development of simple colour tests for the selective detection of H_2O_2 vapours e.g. in peroxide-based explosives.[20]

Experimental Section

Manganese(II) chloride tetrahydrate (AnalaR, 99.5%, BDH), Tiron (1,2-dihydroxybenzene-3,5-disulfonate, disodium salt, monohydrate, Sigma-Aldrich), Calmagite, Orange G (Sigma-Aldrich), Orange II (Fluka), hydrogen peroxide (30% w/w, Sigma-Aldrich), N-2-hydroxyethylpiperazine-N'-3-propane-sulfonic acid (EPPS, Sigma-Aldrich), sodium hydrogen carbonate (AnalaR, Sigma-Aldrich), potassium dihydrogen phosphate (AnalaR, BDH), sodium hydroxide pellets (semiconductor grade, 99%, Sigma-Aldrich) and 2,4,6-tri-tert-butylphenol (Sigma-Aldrich) were used as received. De-ionised water (ELGA Purelab) was used in all experiments and plastic spatuale were used to transfer solid reagents. (Bi)carbonate solutions were made up in boiled water (to remove dissolved CO_2).[21]

Catalytic oxidations of the dyes were carried out at pH 7.5-9.0 and 20±1°C in the presence of an excess of H_2O_2 over dye (~500) so that rates were not influenced by changes in [H_2O_2]. In experiments used for subsequent kinetic analysis the dye:Mn ratio was high (> 20) in order that absorbance readings reflected the concentration of uncomplexed dye thus simplyfing the analysis. A 500 mL four-necked Pyrex container was used that was specially designed to be narrow in the section containing the reaction solution so as to prevent excessive frothing of the dyes. The reaction solution was circulated using a sipper pump (JENWAY) via silicone rubber tubing through a 1 mm glass flow cell housed in a JENWAY 6315 (scanning) UV/VIS spectrophotometer and then back to the reaction vessel. The flow was at a rate such that there was no significant temperature loss between the reaction vessel and the flow cell. The remaining neck on the reaction vessel was left open for the addition of aqueous manganese(II) catalyst; this also ensured that there was no build up of pressure inside the container. In a typical experiment, potassium dihydrogen phosphate (1.00 M, adjusted to pH 8.0 using NaOH(aq), 5.00 mL), aqueous Calmagite (1.00 mM, 5.00 mL) and hydrogen peroxide (0.500 M, 5.00 mL) were added to deionised water ~30 mL). The pH of the solution was adjusted to 8.0±0.1 using freshly prepared (CO_2-free) semi-conductor grade NaOH(aq) and the solution made up to exactly 50.0 mL. The now dark purple reaction solution was transferred to the reaction vessel and the stirrer and pump turned on. $MnCl_2 \cdot 4H_2O$ (5.00 mM, 0.500 mL) was added and readings were commenced. The changes in absorbance of the solution at 540 nm ($\square$ = 10, 500 L mol^{-1} cm^{-1}) were recorded electronically at 10 second intervals. Dilute aqueous HCl was used to adjust the pH of carbonate buffer solutions to pH 9.0.

ESI-MS chromatograms of the bleaching solutions were run on an Agilent 1100 Series LC/MSD Trap.

The EPR experiments in figure 3 and 4 were carried out using a Bruker EMX spectrometer at X-band (~9.5 GHz), equipped with a Bruker ER 4116DM dual mode resonator (9.41 GHz parallel mode, 9.65 GHz perpendicular mode) and with an Oxford Instruments ESR900 cryostat for measurements at cryogenic temperatures 4–10 K.

The EPR measurements in figure 5 were performed using an X/Q-band Bruker Elexsys E580 Spectrometer (Bruker BioSpin GmbH, Germany) equipped with a closed-cycle cryostat (Cryogenic Ltd, UK) and an X-band split-ring resonator module with 2 mm sample access (ER 4118X-MS2). Baseline spectra samples containing only buffer were used for baseline correction; all the spectra presented have been baseline-subtracted.

EPR samples, 100 or 10 µL, contained 100 mM aqueous MnCl2·4H2O mixed with aqueous buffer (either phosphate or carbonate), H2O2 and dye substrate and were flash-frozen and stored in liquid nitrogen (77 K) prior to EPR investigation. The lag time between mixing and freezing was 20 seconds. Experimental conditions are reported in the figures captions.

Acknowledgement

Notes and references

1   G. Strukul, Catalytic Oxidations With Hydrogen Peroxide As Oxidant; Kluwer Academic Publishers, 1993. R. Hage, J. E. Iburg, J. Kerschner, J. H. Koek, E. L. M. Lempers, R. J. Martens, U. S. Racherla, S. W. Russell, T. Swarthoff, M. R. P. Vanvliet, J. B. Warnaar, L. Vanderwolf and B. Krijnen, Nature 1994, 369, 637. R. Noyori, M. Aoki and K. Sato, Chem Commun., 2003, 1977. D. Chandra and A. Bhaumik, Ind. Eng. Chem. Res., 2006, 45, 4879.

2   J. M. Campos-Martin, G. Blanco-Brieva and J. L. Fierro, Angew. Chem. Int. Ed., 2006, 45, 6962.

3   Pollution, Prevention and Abatement Handbook, World Bank Group, Washington D.C., 1998, ISBN 0-8213-3638-X.

4   H. Zollinger, Color Chemistry: Synthesis, Properties and Applications of Organic Dyes and Pigments, Wiley, Weinheim, 3rd edn., 2003.

5   E. S. Beach, R. T. Malecky, R. R. Gil, C. P. Horwitz and T. J. Collins, Catal. Sci. Technol., 2011, 1, 437.

6   G.L. Baughman and E. J. Weber, Environ. Sci. Technol., 1994, 28, 267.

7   E. Ember, S. Rothbart, R. Puchta and R. van Eldik, New J. Chem., 2009, 33, 34.

8   S. Rothbart, E. Ember and R. van Eldik, Dalton Trans., 2010, 39, 3264.

9   S. Rothbart, E. Ember and R. van Eldik, New J. Chem., 2012, 36, 732.

10   D. Swern, Organic Peroxides, Wiley, New York, 1970, pp. 313.

11   V. Nadtochenko and J. Kiwi, J. Chem. Soc., Faraday Trans., 1997, 93, 2373.

12   J. Griffiths, J. Soc. Dyers Colour., 1971, 801; 1972, 106.

13   T. S. Sheriff, S. Cope and M. Ekwegh, Dalton Trans., 2007, 5119.   T. S. Sheriff, S. Cope and D.S. Varsani, Dalton Trans., 2013, 42, 5673.

14   M. G. Evan and N. Uri, Trans. Faraday Soc., 1949, 45, 224.

15   T.S. Sheriff, J. Chem. Soc., Dalton Trans., 1992, 1051.

16   K.A. Campbell, M.R. Lashley, J.K. Wyatt, M.H. Nantz and R.D. Britt, J. Am. Chem. Soc., 2001, 123, 5710.

17   J. Oakes, P. Gratton and I. Weil, J. Chem. Soc., Dalton Trans., 1997,   3805.

18   C. A. Wegermann, P. Strapasson, S. M. M. Romanowski, A. Bortoluzzi, R. R. Ribeiro, F. S. Nunes and S. M. Drechsel, App. Cat A: Gen., 2013, 454, 11.

19   O. Abollino, C. Sarzanini and E. Mentasti, Talanta, 1994, 41, 1107.

20   T.S. Sheriff, S. Miah and K. L. Kuok, RSC Adv., 2014, 4, 35116.

21   G.E. Delroy and E.J. King, Biochem., 1945, 39, 245.

[a]UG 4th year chemistry MSci project students, Department of Chemistry and Biochemistry, Queen Mary University of London, London E1 4NS, UK. [b] EPR Research Facility Fellow, School of

Biological and Chemical Science, Queen Mary University of London, Mile End Road, E1 4NS London, UK and London Centre for Nanotechnology, UCL, 17-19 Gordon Street, WC1H 0AH London, UK. E-mail: e.salvadori@qmul.ac.uk, [c]Inorganic Research Laboratories, The Joseph Priestley Building, Department of Chemistry and Biochemistry, Queen Mary University of London, London E1 4NS, UK. Tel: 020 7882 8466; Fax: 020 7882 3239. E-mail: t.s.sheriff@qmul.ac.uk

†Electronic Supplementary Information (ESI) available:
ESI1 Log-log plot of initial rate of CAL bleaching vs [MnII];
ESI2 Log-log plot of initial rate of CAL bleaching vs [H2O2];
ESI3 Log-log plot of initial rate of CAL bleaching vs [CAL];
ESI4 X-band EPR spectra of MnCl2·4H2O (100 □M) at pH 8.0 or pH 9.0 and after the addition of H2O2.
ESI5 ESI-MS chromatograms of CAL at pH 8.0 (phosphate buffer) and CAL at pH 8.0 (phosphate buffer) with added MnCl2·4H2O;
ESI6 Log-log plot of initial rate of O II and O G bleaching vs [MnII];
ESI7 Log-log plot of initial rate of O II and O G bleaching vs [H2O2];
ESI8 Log-log plot of initial rate of O II and O G bleaching vs [HCO3–];
ESI9 X-band EPR spectra of MnCl2·4H2O (100 □M), H2O2 (50.0 mM) and O II (0.100 mM) at pH 9.0 (50 mM, carbonate buffer).
ESI10 X-band EPR spectra of MnCl2·4H2O (100 □M) and with H2O2 (50.0 mM) or O II (0.100 mM) or both H2O2 (50.0 mM) and O II (0.100 mM) at pH 9.0 (50 mM, carbonate buffer).
ESI11 Change in absorbance maxima of O II and O G on addition of MnCl2·4H2O;
ESI12 The change in absorbance of CAL at pH 8.0 (phosphate buffer) and O II at pH 9.0 (carbonate buffer) with time after successive additions of dye with added MnCl2·4H2O].